

Process Simulation and Optimization of Adipic Acid Catalytic Ammoniation for Adiponitrile Production

Peng Jia^{1,*}, Song Xue¹, Yuhan Yan², Qi Zhang¹, Yanhong Huang³, Pengzhi Bei¹, Zian Yan¹, Xu Feng¹, Yifan Zhang¹, Qianqian Xu¹

¹School of Petrochemical Engineering, Shenyang University of Technology, Liaoning, China

²Department of General Foreign Language Teaching, Liaoyang Vocational College of Technology, Liaoning, China

³Technical Research Department, Binzhou Special Equipment Inspection Institute, Shandong, China

*Corresponding author: jiapeng_1988@163.com

Abstract: Adiponitrile (ADN) is a critical raw material for nylon 66, and its efficient, green production is vital for securing the supply chain of key materials. Among domestic ADN production methods, the traditional butadiene hydrocyanation process faces challenges such as complex procedures, high energy consumption, and significant safety risks. In contrast, the adipic acid (AA) ammoniation method has garnered attention due to its simplified process, high product yield, and relatively low investment. However, industrial applications still encounter technical bottlenecks, including excessive energy consumption and insufficient heat integration. This study focuses on optimizing the AA ammoniation process for ADN production using Aspen Plus simulation, process intensification, and heat integration technologies. A comprehensive process model was developed, covering key units such as reactors and distillation columns. Sensitivity analysis was employed to investigate parameters like theoretical tray numbers, reflux ratios, and feed positions, revealing significant energy consumption in the cyclopentanone purification column (T0306). By introducing heat pump distillation technology, the latent heat of top vapors was recovered to drive the reboiler, reducing energy consumption by 85.9%. Additionally, the heat exchanger network was optimized by removing small-area exchangers and breaking loop circuits, achieving an 18.84% reduction in energy consumption. This research provides theoretical and technical support for the industrial development of green ADN production processes.

Keywords: Adiponitrile; Adipic acid ammoniation; Sensitivity analysis; Process energy-saving optimization; Heat exchanger network optimization.

1. Introduction

Adiponitrile (ADN), a critical precursor for Nylon 66 production, is widely utilized in automotive lightweighting (e.g., engine components, airbags), electronics (connectors, insulating materials), and specialty fibers (military, aerospace) due to its exceptional strength, heat resistance, and chemical stability [1, 2]. Global demand for Nylon 66 has surged, surpassing 3 million tons in 2023, with China accounting for over 35% of total consumption [3]. Despite this, China's ADN production remains heavily import-dependent, with an import reliance rate exceeding 90% as of 2022, primarily sourced from international giants like Invista and Ascend, posing significant supply chain risks [4].

Currently, three industrial routes dominate ADN production:

(1) Butadiene Hydrocyanation (BD Process): Mature and high-yield (>95%), this method relies on high-purity butadiene and toxic hydrogen cyanide (HCN), with core technologies monopolized by Invista and BASF. However, its dependence on hazardous HCN raises safety concerns in storage, transportation, and disposal [5-7].

(2) Acrylonitrile Electrolysis (AN Process): Patented by Asahi Kasei, this energy-intensive process consumes ~5,000 kWh per ton of ADN and faces challenges with ammonium sulfate byproduct pollution [8].

(3) Adipic Acid Ammoniation (AA Process): Utilizing adipic acid (AA) and liquid ammonia under moderate conditions, this method offers simplicity and high product quality. However, issues like excessive energy consumption, byproduct generation, and economic inefficiency limit its

global capacity share to <5% [9].

Recent domestic advancements in butadiene-based ADN production (e.g., by Huafon Group and China National Chemical Engineering Tianchen Yaobang) remain constrained by reliance on imported catalysts and volatile butadiene prices. In 2024, butadiene prices fluctuated drastically, with an amplitude of 60.17%, escalating from 8,000–9,000 to 13,000–14,000 CNY/ton, further inflating costs [10]. Concurrently, China's AA market experienced a downward trend in 2024, with prices ranging from 7,700 to 10,500 CNY/ton, driven by oversupply [11]. These dynamics underscore the urgency to reevaluate the AA process's technological potential for diversifying production routes and enhancing supply chain resilience.

The industrial application of the AA ammoniation method faces persistent challenges:

(1) Low Reaction Efficiency: Under high-temperature, high-pressure conditions (200–300°C, 5–10 MPa), poor selectivity leads to substantial byproducts like adipamide (ADM) and AA ammonium salts, restricting ADN yields to <80% [12].

(2) High Energy and Carbon Footprint: Continuous external heating and steam separation account for >40% of total energy consumption, with CO₂ emissions reaching 4.5–5.2 tons per ton of ADN, significantly exceeding those of the BD process (3.0–3.8 tons) [13].

Despite these limitations, the AA process has garnered renewed interest due to its inherent advantages: simplified workflows, high product purity, and lower capital investment. China's AA overcapacity—exceeding 3 million tons in 2024 with an operational rate below 60%—presents a strategic

opportunity to transform surplus AA into high-value ADN, aligning with resource utilization and industrial upgrading goals [14]. By addressing technical bottlenecks through process optimization, this method could emerge as a sustainable alternative, balancing economic viability with environmental compliance.

The global ADN manufacturing landscape has been predominantly shaped by two established methodologies: butadiene hydrocyanation (Butene route) and acrylonitrile electrodimmerization (AN process) [15]. Leading corporations including Invista (USA) and Asahi Kasei (Japan) have achieved remarkable yield enhancements exceeding 95% through catalytic system innovations and reactor configuration optimizations in Butene-based processes. Nevertheless, these advancements remain constrained by dependence on precious metal catalysts and intricate byproduct management [16, 17]. Recent exploratory efforts by BASF involve developing an alternative approach through direct amination of adipic acid (AA), demonstrating continuous production under mild conditions ($\approx 92\%$ yield) via fixed-bed reactors. However, commercialization challenges persist due to intense exothermic reactions during amination and energy-intensive product purification.

Regarding distillation intensification, vapor recompression (VRC) technology has been widely implemented in European petrochemical operations. Notable applications include Linde AG's 40-50% energy reduction in propylene-propane separation [18]. Academic contributions, such as Universität Dortmund's parametric optimization of double-effect distillation for ethanol dehydration, have shown significant steam consumption reduction [19]. Current research predominantly focuses on individual distillation columns, with limited exploration of thermodynamic synergy in multi-column configurations.

In thermal integration research, pinch analysis pioneered by Linnhoff at the University of Manchester has been successfully deployed in Shell's refinery operations [20]. MIT researchers have advanced multi-objective optimization algorithms combining evolutionary computation with reinforcement learning for heat exchanger network design. Despite theoretical progress, computational complexity hinders practical industrial implementation [21].

China's ADN production capacity has historically relied on imports, though recent breakthroughs by Sinopec in Butene process localization have narrowed technological gaps. Persistent challenges remain in energy efficiency and production costs compared to international benchmarks [22]. Tianchen Engineering's innovative two-step esterification-

amination route achieves 98% ADN yield but encounters high methanol consumption and energy-intensive distillation accounting for $>60\%$ of total expenditure. Tsinghua University's reactive distillation integration strategy reduces intermediate separation requirements, yet material corrosion from high-temperature amination reactions remains unresolved [23, 24].

Zhejiang University researchers have developed hybrid heat pump-thermal integration systems demonstrating 35% energy savings in methanol-water separation. Their response surface methodology optimization achieved 99.2% ethyl acetate purity, though ADN-related distillation intensification for high-boiling systems remains laboratory-scale [25]. East China University of Science and Technology's staged waste heat recovery strategy improved low-grade thermal energy utilization in coal chemical processes [26]. Current methodologies predominantly address unit operations individually, lacking holistic optimization across reaction-separation-heat exchange systems. Key limitations include: Suboptimal energy distribution between reaction and separation units in AA amination processes; Underexplored energy cascading in multi-column systems; Inadequate multivariate optimization beyond conventional single-parameter sensitivity analysis.

This study addresses these gaps through integrated process modeling, multi-criteria parameter optimization, and systematic thermal integration design, aiming to establish an energy-efficient ADN production framework with industrial applicability. The proposed methodology provides theoretical foundations and practical solutions for sustainable adiponitrile manufacturing.

2. Reaction Mechanism and Kinetic Modeling

2.1. Ammoniation Reaction Kinetics

Based on the bimolecular mechanism proposed by Rhône-Poulenc, the neutralization of adipic acid (AA) with two ammonia molecules forms a diammonium salt. This intermediate undergoes dehydration to yield either a cyanammonium salt or adipamide, followed by sequential water elimination to ultimately produce adiponitrile (ADN). The dehydration of ammonium salts to amides proceeds without a catalyst, whereas further dehydration of amides to ADN necessitates catalytic intervention to suppress side reactions [27], as illustrated in Fig. 1.

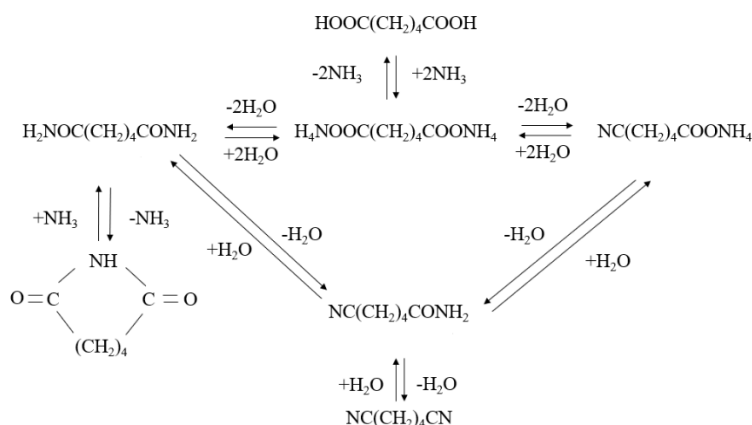
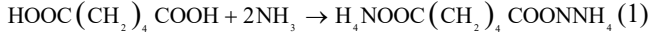


Figure 1. Rhône-Poulenc Adiponitrile Synthesis Mechanism

Main Reaction Pathway:



AA reacts with ammonia to form an ammonium salt, which dehydrates into an amide. The ammonium salt and adipamide equilibrate to some extent. The overall reaction involves neutralization of two ammonia molecules and elimination of two water molecules. Since the dehydration of the ammonium salt to adipamide is non-catalytic and concurrent with neutralization, these steps are combined into a consolidated reaction:



This irreversible neutralization reaction follows power-law kinetics. According to Feng et al., the macro-kinetics depend on acid concentration: first-order when AA concentration exceeds 2 mol/L and second-order below this threshold [28]. Pre-exponential factors are referenced to reactor volume (units: m³). Rate constants (k_1 and k_2) at varying temperatures, derived via linear least-squares regression of literature data, are summarized in Table 1.

The section headings are in boldface capital and lowercase letters. Second level headings are typed as part of the succeeding paragraph (like the subsection heading of this paragraph). All manuscripts must be in English, also the table and figure texts, otherwise we cannot publish your paper. Please keep a second copy of your manuscript in your office.

Table 1. Macro-Kinetic Rate Constants at Different Temperatures

T/K	K_1/min^{-1}	$R^2(k_1)$	K_2/min^{-1}	$R^2(k_2)$
483.2	0.0517	0.9914	0.3424	0.9941
493.2	0.0713	0.9864	0.3894	0.9835
503.2	0.0845	0.9903	0.4765	0.9887
513.2	0.1132	0.9969	0.6082	0.9845
523.2	0.1509	0.9977	0.7381	0.9963
533.2	0.1833	0.9996	1.0571	0.9901

The Arrhenius equation, was fitted to derive activation energies and pre-exponential factors, as shown in Table 2.

Table 2. Macro-Kinetic Apparent Pre-exponential Factor

	$K_0(\text{min}^{-1})$	$E_a(\text{J}\cdot\text{mol}^{-1})$
First-order reaction	2.58×10^3	4.29×10^4
Second-order reaction	1.50×10^5	5.27×10^4

The first-order reaction kinetics is:

$$r_1 = 43 \exp\left(-\frac{4.29 \times 10^4}{RT}\right) CBL_1 \quad (4)$$

The Second-order reaction kinetics is:

$$r_2 = k_2 \exp\left(-\frac{E_{a2}}{RT}\right) CBL_2 \quad (5)$$

Side Reaction Pathway:

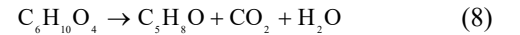
(1) AA ammonolysis to adipimide and water:



(2) Adipimide conversion to adipamide:



(3) AA decomposition to cyclopentanone, CO₂, and water:



Due to insufficient kinetic data for side reactions, a side reactor was connected in series to simulate these pathways using predefined conversions (Table 3). Adjustments were made to align simulated product distributions with patent-reported yields [29].

Table 3. Side Reaction Conversion

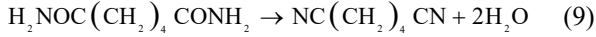
Reaction	Conversion	Converted Component
$\text{C}_6\text{H}_{10}\text{O}_4 + \text{NH}_3 \rightarrow \text{C}_6\text{H}_9\text{NO}_2 + 2\text{H}_2\text{O}$	0.001	$\text{C}_6\text{H}_{10}\text{O}_4$
$\text{C}_6\text{H}_9\text{NO}_2 + \text{NH}_3 \rightarrow \text{C}_6\text{H}_{12}\text{N}_2\text{O}_2$	0.6	$\text{C}_6\text{H}_9\text{NO}_2$
$\text{C}_6\text{H}_{10}\text{O}_4 \rightarrow \text{C}_5\text{H}_8\text{O} + \text{CO}_2 + \text{H}_2\text{O}$	0.02	$\text{C}_6\text{H}_{10}\text{O}_4$

2.2. Nitrilation Reaction Kinetics

The dehydration of adipamide eliminates one water

molecule to form δ -cyanovaleramide, which subsequently undergoes further dehydration to yield ADN [30]. Both dehydration steps are reversible, with δ -cyanovaleramide

equilibrating with ADN. These reactions require phosphoric acid (H_3PO_4) as a catalyst to achieve optimal dehydration efficiency. Given their simultaneous progression, the two steps are consolidated into a single overall reaction:



This irreversible dehydration follows power-law kinetics. Studies by Gao et al. demonstrate that phosphoric acid significantly accelerates the reaction rate. At constant temperature and initial AA concentration, increasing catalyst concentration reduces AA concentration more rapidly within 5 minutes; however, beyond 0.2% H_3PO_4 , the effect plateaus [31]. Thus, industrial processes optimize H_3PO_4 concentration at 0.2%.

Based on Zhang’s work [32], the dehydration rate is proportional to the unreacted fraction. Let the dehydration rate (α) be defined as:

$$\frac{d\beta_r}{dt} = k(1 - \beta_r) \quad (10)$$

Phosphoric acid lowers the activation energy of dehydration. The relationship is expressed as:

$$k = A \exp\left(\frac{-[E + B_1 \exp(-aC_p)]}{RT}\right) \quad (11)$$

Incorporating Zhang’s data [32], the kinetic equation becomes:

$$r_3 = 1.03 \times 10^8 \exp\left\{\frac{-[23.6 + 2.07 \exp(-644C_p)] \times 10^3}{RT}\right\} \quad (12)$$

2.3. Preliminary Process Overview

This chapter outlines the production of purified adiponitrile

(ADN) using adipic acid (AA) and ammonia as raw materials. Key process equipment—including reactors, distillation columns, heat exchangers, compressors, and flash drums—are analyzed. Sensitivity tools in Aspen Plus are employed to optimize critical parameters (e.g., reactor selection, kinetic models, reaction temperature, and distillation conditions) for initial tuning, followed by comprehensive process simulation and refinement.

Fresh liquid ammonia is mixed with recycled liquid ammonia and fed into a vaporizer. The vaporized stream is heated and introduced into the amidation reactor (R0101). Meanwhile, fresh AA is blended with phosphoric acid catalyst, recycled AA, and recycled semi-nitrile solution, preheated in an AA heater, and directed to the amidation reactor. Within R0101, the primary intermediate, adipamide, is formed. The gaseous effluent from R0101 enters a gas-liquid separator, where ammonia gas is compressed, reheated, and routed to the nitrilation reactor (R0202). The liquid effluent from R0101 and the separator is combined, heated, and fed into R0202. Here, dehydration reactions yield the final ADN product.

The nitrilation reactor effluent is sent to the ammonia removal column (T0301). The column overhead, containing trace water, ammonia, and CO_2 , enters an ammonia decarbonation column (T0307) to recover recycled ammonia and isolate CO_2 . The T0301 bottoms are transferred to a dehydration column (T0302), where wastewater is removed overhead. The column bottoms, containing ADN and heavy components, proceed to a crude ADN heavy removal column. Heavy residues rich in AA are sent to an AA recovery column (T0303) for AA recycling, while the overhead crude ADN is purified in an ADN refining column (T0304).

The T0304 bottoms yield 99.86 wt% pure ADN and recycled semi-nitrile solution. The overhead crude cyclopentanone stream enters a cyclopentanone refining column (T0305), where heavy waste is removed from the bottoms. The overhead aqueous cyclopentanone is further purified in a cyclopentanone purification column (T0306). The T0306 bottoms produce byproduct cyclopentanone, while the overhead discharges wastewater.

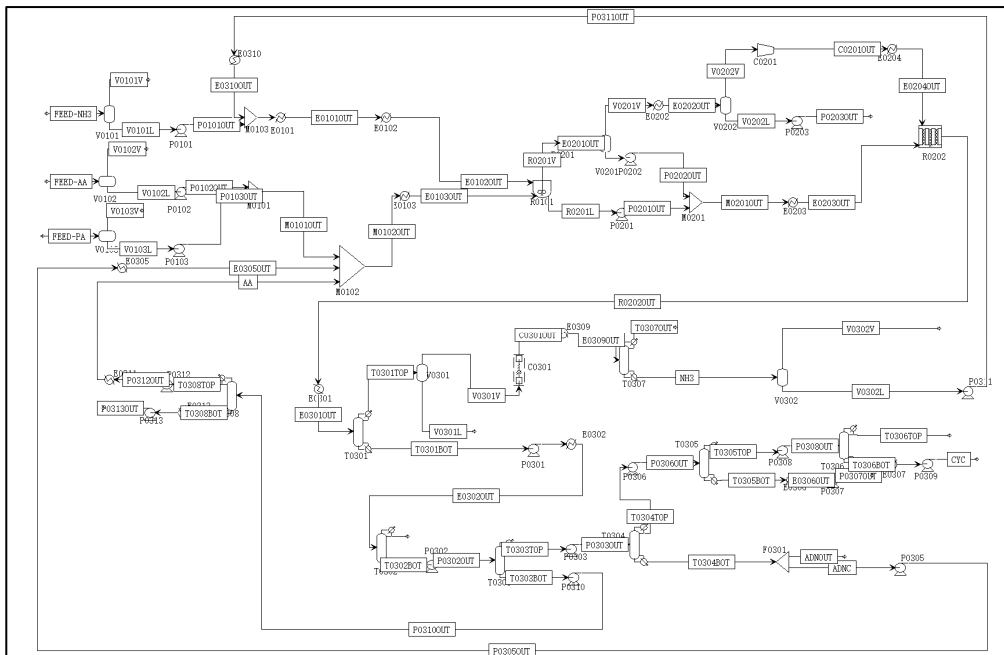


Figure 2. Full-Process Simulation (No Energy-Saving, No Heat Exchange)

3. Optimization of Key Parameters in Distillation Processes

3.1. T0303 Heavy Component Separation Columns

To further separate residual heavy components from the dehydration column, isolating unreacted adipic acid (AA) from adiponitrile (ADN). The goal is to maximize ADN purity in the overhead stream while minimizing ADN content in the bottoms for subsequent transfer to the ADN refining column.

In Fig. 3, as the theoretical plate count increases, the ADN mass flow rate at the column bottoms progressively decreases. At 40 plates, the mass flow rate drops from 13,000 kg/hr to near 0 kg/hr. Thus, the optimized plate count for T0303 is 41 plates, achieving maximum ADN mass flow in the overhead stream.

In Fig. 4, the ADN mass flow rate at the bottoms initially decreases, stabilizes, and then rises with higher feed tray positions. To prevent ADN loss to the bottoms, the feed tray is positioned above tray 22.

In Fig. 5, increasing the molar reflux ratio reduces ADN content in the bottoms. At a reflux ratio of 0.25, ADN is fully excluded from the bottoms, maximizing overhead ADN purity.

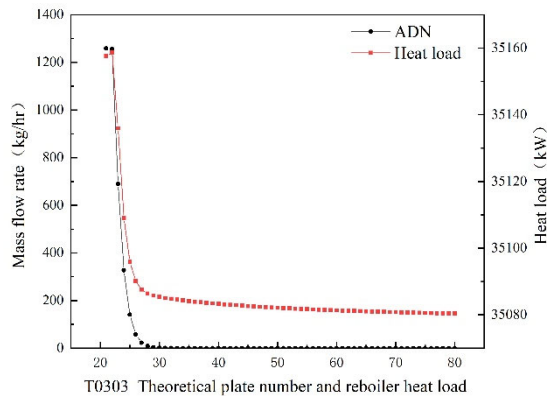


Figure 3. Sensitivity Analysis of Theoretical Plate Number and Reboiler Heat Duty for T0303

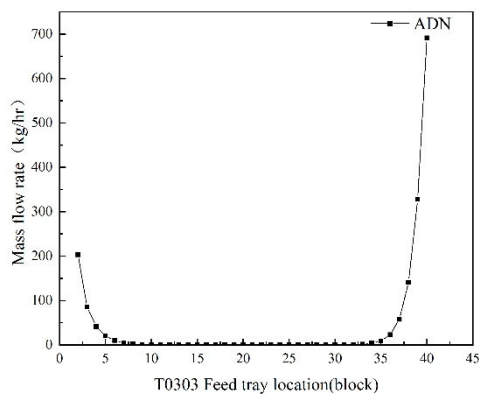


Figure 4. Sensitivity Analysis of Feed Tray Position for T0303

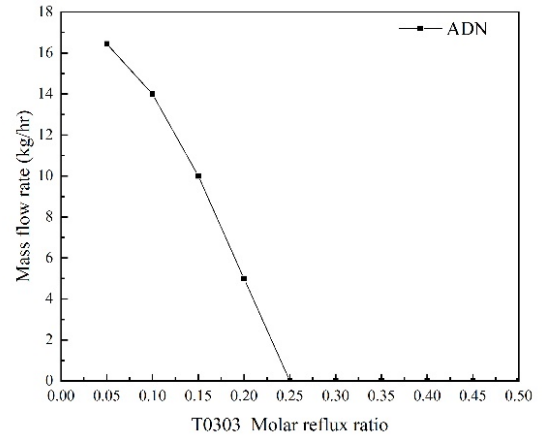


Figure 5. Sensitivity Analysis of Molar Reflux Ratio for T0303

3.2. T0304 Dehydration Column

To separate water from ADN-heavy components in the ammonia removal column bottoms, discharging wastewater to treatment facilities while retaining ADN in the bottoms.

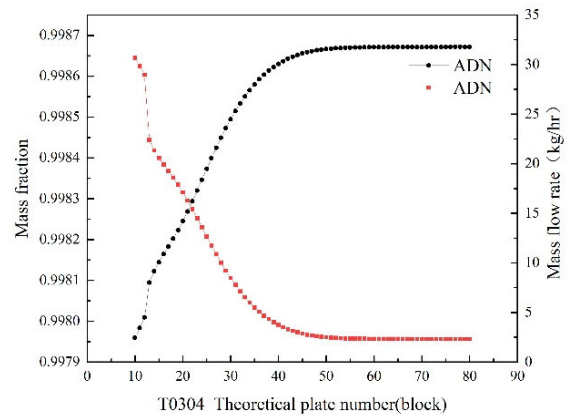


Figure 6. Sensitivity Analysis of Theoretical Plate Number for T0304

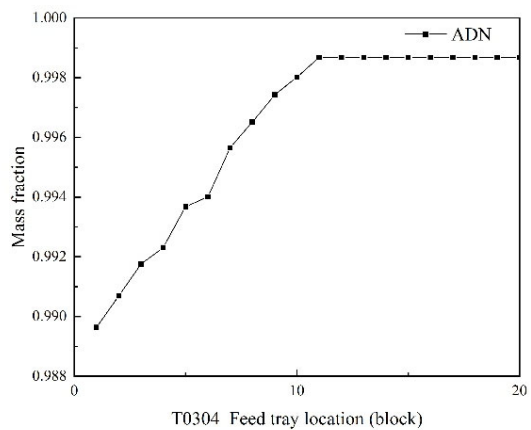


Figure 7. Sensitivity Analysis of Feed Tray Position for T0304

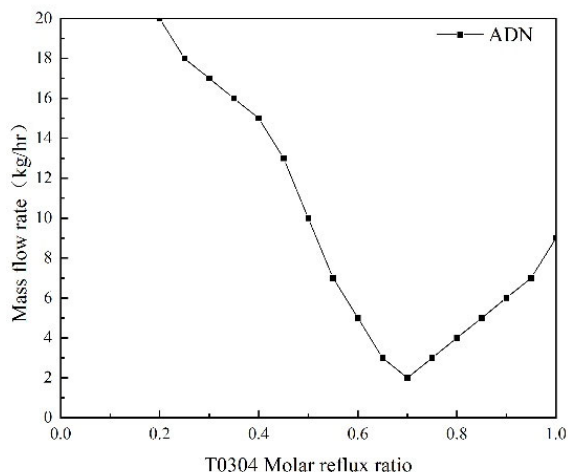


Figure 8. Sensitivity Analysis of Molar Reflux Ratio for T0304

In Fig. 6, higher plate counts reduce ADN mass flow in the overhead while increasing both mass flow and purity of ADN in the bottoms. Stability is achieved beyond 55 plates. To enhance water-ADN separation efficiency, 72 plates are selected.

In Fig. 7, the overhead ADN mass flow initially rises and stabilizes at a feed tray position above tray 11. To minimize ADN loss, the feed tray is positioned above tray 12.

In Fig. 8, the overhead ADN mass flow exhibits an initial increase followed by a decline with higher reflux ratios. A reflux ratio of 0.7 is chosen to limit ADN in the overhead.

3.3. T0308 Adipic Acid Recovery Column

To separate water from ADN-heavy components in the ammonia removal column bottoms, discharging wastewater to treatment facilities while retaining ADN in the bottoms.

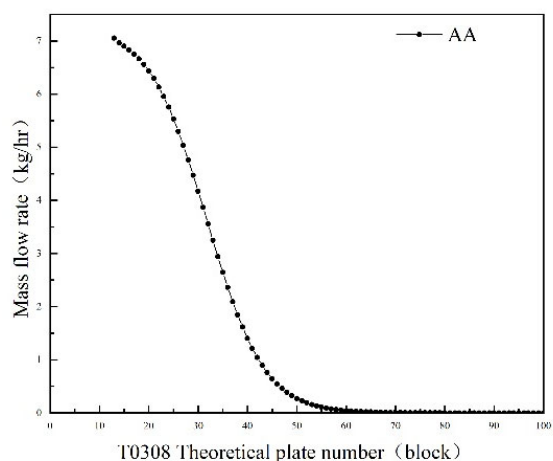


Figure 9. Sensitivity Analysis of Theoretical Plate Number for T0308

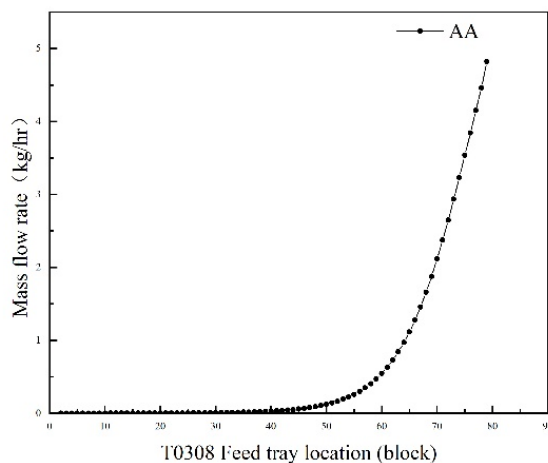


Figure 10. Sensitivity Analysis of Feed Tray Position for T0308

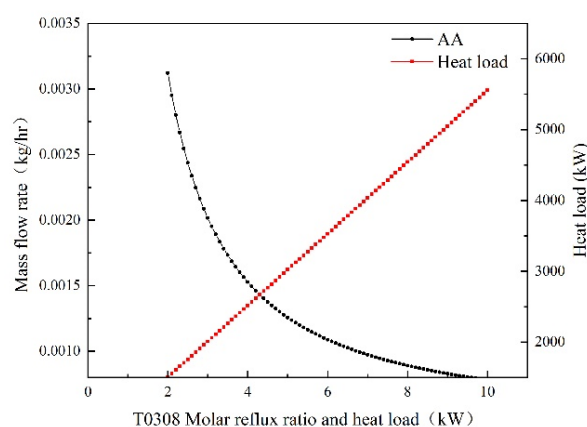


Figure 11. Sensitivity Analysis of Molar Reflux Ratio, Mass Flow Rate of Adipic Acid, and Reboiler Heat Duty for T0308

In Fig. 9, increasing plates reduces AA mass flow in the bottoms while enhancing overhead purity. Stability is observed beyond 70 plates. 80 plates are selected to maximize AA recovery efficiency.

In Fig. 10, higher feed tray positions increase AA content in the bottoms. To minimize AA loss, the feed tray is positioned above tray 13.

In Fig. 11, higher reflux ratios reduce AA in the bottoms but increase reboiler heat duty. A reflux ratio of 7 balances economic and energy considerations.

4. Optimization of Energy-Saving Technologies

4.1. Extraction of Original Process Streams

For heat exchanger network (HEN) design and optimization, initial process stream data were extracted, and redundant streams/equipment were eliminated to simplify the system. The original HEN was analyzed using composite and grand composite curves to identify energy recovery potential. Heat pump distillation (HPD) was introduced to reduce phase-change platform overlap and enhance energy utilization [33]. Integration of Aspen Plus V11 and Aspen Energy Analyzer V11 enabled systematic optimization.

Table 4. Process Stream Information (Original Process Streams)

Stream ID	Type	Inlet/°C	Outlet/°C	Heat Duty/kW
C0201OUT_To_E0204OUT	Cold	97.76	300	2919.49
M0102OUT_To_E0103OUT	Cold	193.56	260	2144.67
M0201OUT_To_E0203OUT	Cold	200.54	300	3477.92
P0311OUT_To_E0310OUT	Cold	-15.56	-6.80	271.51
M0103OUT_To_E0102OUT	Cold	-8.10	260	13004.38
P0312OUT_To_AA	Hot	307.78	180	335.04
R0201V_To_E0201OUT	Hot	250.00	118.8	6631.10
R0202OUT_To_E0301OUT	Hot	275.00	83.79	41330.42
T0308OUT_To_E0313OUT	Hot	420.19	25	25.06
P0305OUT_To_E0305OUT	Hot	309.80	200	2572.41
T0306BOT_To_E0307OUT	Hot	141.49	25	1.61
V0201V_To_E0202OUT	Hot	118.48	19.41	3303.85
T0305BOT_To_E0306OUT	Hot	244.15	25	5044.53
C0301OUT_To_E0309OUT	Hot	80.00	10	7979.79
P0301OUT_To_E0302OUT	Hot	153.29	110	2282.82

Table 5. Column Stream Information (Original Process Streams)

Column ID	Exchanger Type	Inlet/°C	Outlet/°C	Heat Duty/kW
T0308	Condenser	307.54	307.43	4056.34
T0304	Condenser	193.47	108.51	41619.48
T0303	Condenser	263.96	207.04	37464.76
T0307	Condenser	27.98	-1.01	2068.13
T0306	Condenser	104.94	104.83	2040.63
T0302	Condenser	104.91	104.83	5246.87
T0305	Condenser	110.93	109.94	8828.39
T0301	Condenser	52.51	-3.23	3822.98
T0308	Reboiler	350.28	420.19	4036.79
T0304	Reboiler	309.56	309.66	42318.59
T0307	Reboiler	49.07	49.12	3537.80
T0303	Reboiler	314.28	315.46	35082.98
T0302	Reboiler	194.41	259.44	12644.11
T0306	Reboiler	139.69	141.49	2040.18
T0301	Reboiler	131.37	153.26	5688.64
T0305	Reboiler	243.13	244.15	11825.89

4.2. Energy Consumption Analysis of Original Process Streams

The impact of minimum temperature difference (ΔT_{min}) on system economics was evaluated, revealing the relationship between total cost and ΔT_{min} (Fig. 12).

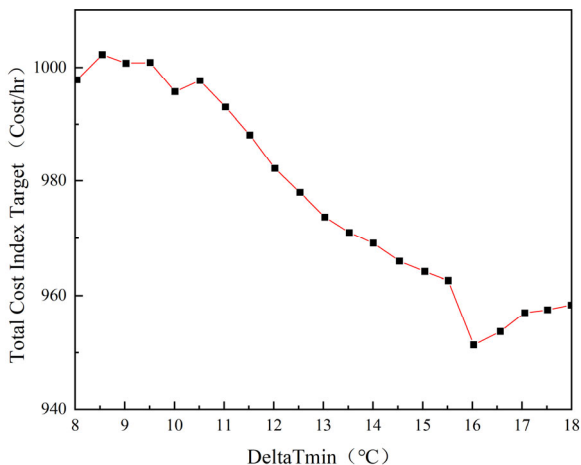


Figure 12. Relationship Curve of Total Cost-Minimum Heat Transfer Temperature Difference

The pinch temperature difference (ΔT_{min}) is a critical parameter in heat exchanger network (HEN) synthesis. A smaller ΔT_{min} enhances heat recovery potential, thereby reducing heating and cooling utility demands and operational energy costs. However, excessively low ΔT_{min} values necessitate larger heat transfer areas, escalating capital expenditures. Consequently, an optimal ΔT_{min} exists under given process and economic constraints, minimizing total system costs. HEN synthesis should prioritize this value for balanced energy efficiency and cost-effectiveness.

As illustrated in Fig. 12, total costs decrease with increasing ΔT_{min} within the 8-16°C range. This trend arises because larger ΔT_{min} thresholds eliminate numerous small-area exchangers between thermally adjacent streams, reducing capital expenses. Beyond 16°C, costs rise slightly (16-17°C) due to diminishing feasible stream-to-stream heat recovery, followed by stabilization (17-18°C) as most streams rely on external utilities [34].

In practice, overly small ΔT_{min} values (e.g., 5°C) lead to impractical exchanger sizes and operational inflexibility, while excessive ΔT_{min} (e.g., 20°C) compromises energy savings. To address this, $\Delta T_{min} = 16^\circ\text{C}$ was selected as the optimal compromise, achieving substantial energy recovery without prohibitive capital costs. This value aligns with typical industrial heat transfer conditions, ensuring robust

operational flexibility. The corresponding process composite and grand composite curves under this ΔT_{min} are shown in Fig. 13 and 14, respectively.

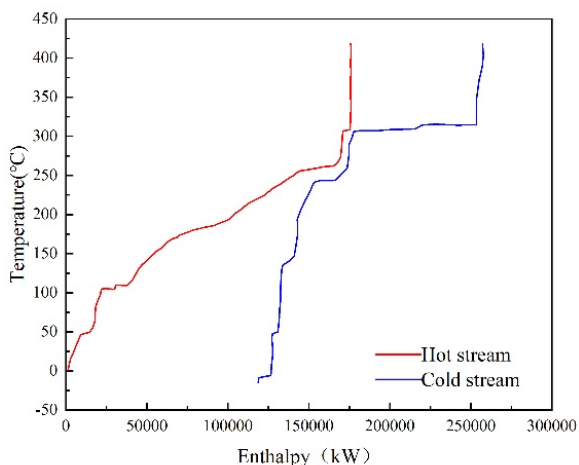


Figure 13. Process Composite Curve (Original Process Streams)

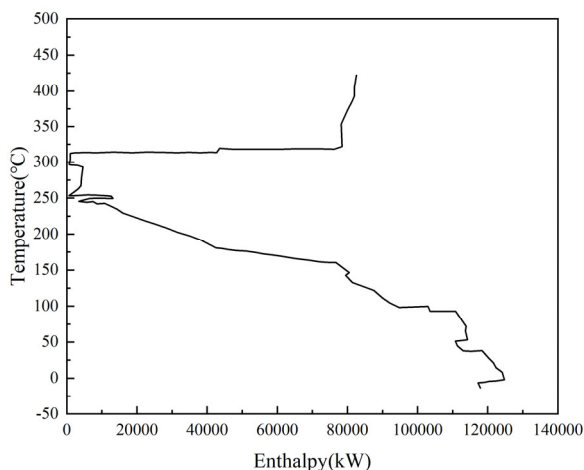


Figure 14. Grand Composite Curve (Original Process Streams)

As depicted in the composite curve (Fig. 13), the thermal platform exhibits substantial energy content but insufficient temperature driving force to meet the minimum heat transfer temperature difference (ΔT_{min}), severely limiting recoverable heat. To address this, modifying the vaporization temperatures of process streams can shift the thermal platforms, enabling enhanced energy recovery through "platform staggering" [34]. Consequently, heat pump technology is employed to upgrade low-grade heat by converting mechanical work into thermal energy. This elevates stream temperatures, facilitating heat exchange between previously incompatible streams and reducing utility consumption.

By integrating heat pumps, minimal additional thermal energy input achieves significant reductions in both heating and cooling demands, yielding substantial energy savings. This approach aligns with industrial feasibility, as it circumvents impractical ΔT_{min} requirements while maximizing latent heat utilization.

4.3. Heat Pump Distillation (HPD) Technology

Heat Pump Distillation (HPD) leverages thermodynamic principles to upgrade low-grade thermal energy into high-grade heat, providing energy-efficient and environmentally sustainable solutions for distillation processes [35]. Compared to conventional distillation, HPD offers distinct advantages:

- (1) **Energy Savings:** By converting low-grade heat (e.g., waste heat or renewable sources) into usable high-temperature heat, HPD reduces reliance on fossil achieving up to 30% energy savings in low-temperature operations;
- (2) **Emission Reduction:** Substitution of coal/oil-derived energy mitigates CO_2 , NO_x , and other pollutant emissions, aligning with decarbonization goals;
- (3) **Enhanced Efficiency:** The thermal efficiency of HPD systems reaches 1.8 that of traditional methods, with energy utilization rates exceeding 85%;
- (4) **Operational Flexibility:** Modular design enables dynamic parameter adjustments ($\pm 15\%$ range), accommodating diverse boiling-point systems through real-time feedback control.

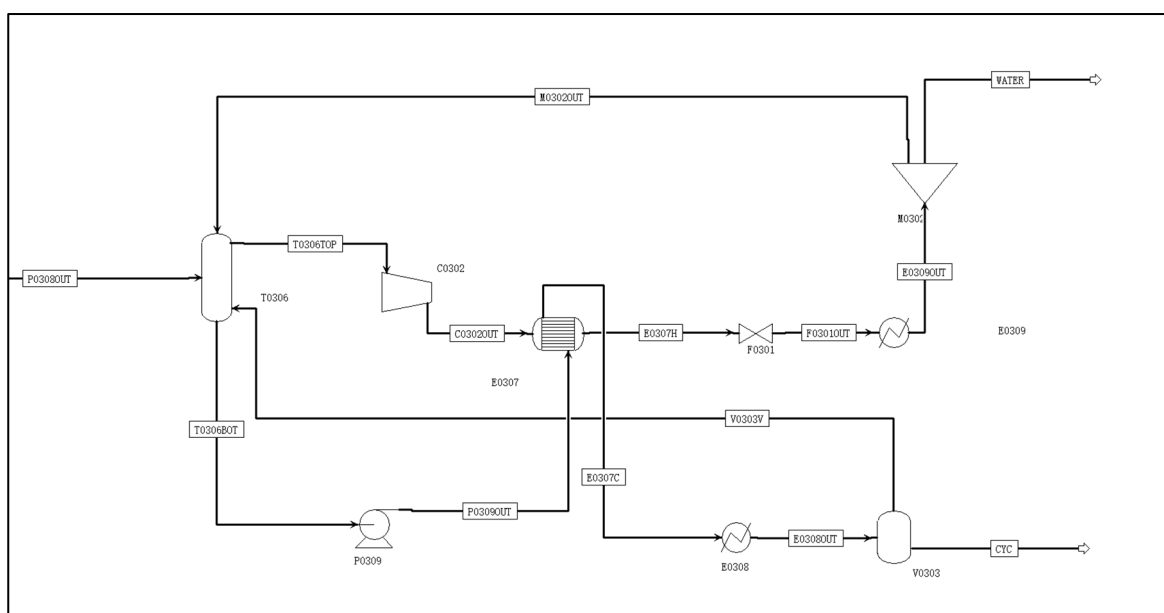


Figure 15. Schematic Diagram of Heat Pump Distillation

The temperature difference between the column top and bottom of T0306 is 37.4°C, with significant latent heat demand. Conventional distillation achieves separation but incurs high energy costs. Implementing HPD, the overhead vapor is compressed and exchanged with the bottom liquid to drive reboiling. The vapor is subsequently condensed and partially withdrawn, drastically reducing energy consumption per column.

The HPD configuration (illustrated in Fig. 15) integrates compression and heat exchange to minimize utility requirements while maintaining separation efficiency.

Incorporating compressor power and cooler energy consumption in Table 6, HPT reduces total energy demand by 3504.6 kW, achieving an 85.9% energy saving compared to the conventional process. Specifically, HPT decreases heating and cooling utility consumption by 85.9% and 86.5%, respectively.

Table 6. Comparison of Processes With and Without Heat Pump Technology

Parameter	Conventional Process (Without HPT)	Heat Pump Technology (HPT)
Cooling Utility (kW)	2040.63	287.5
Heating Utility (kW)	2040.09	275.5
Compressor Power (kW)	0	13.4
Total Energy (kW)	4080.7	576.1

4.4. Heat Exchanger Network Design and Optimization

The process streams were re-imported into Aspen Energy

Analyzer V11 for economic evaluation of the minimum heat transfer temperature difference (ΔT_{min}). The updated total cost vs. ΔT_{min} relationship is shown in Fig. 16.

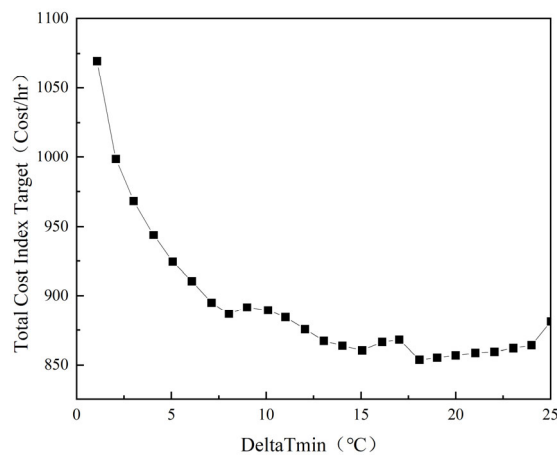


Figure 16. Relationship Curve of Total Cost vs. Minimum Heat Transfer Temperature Difference

A smaller ΔT_{min} increases heat recovery but escalates capital costs due to larger heat exchanger areas, while a larger ΔT_{min} reduces heat recovery efficiency. The optimal ΔT_{min}

of 18°C minimizes total costs (Fig. 16), yielding the energy targets for the heat integration process (Fig. 17):

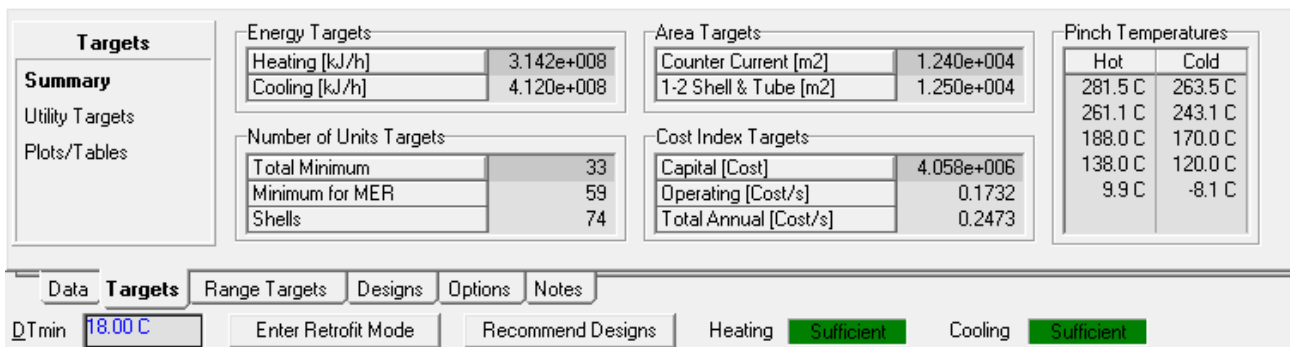


Figure 17. Energy Targets for the Heat Integration Process

As shown in Fig. 17, the theoretical minimum energy requirements for the heat-integrated process are 133,800 kW of heating utility and 206,200 kW of cooling utility. Following heat pump distillation (HPD) optimization, the

process composite curve (Fig. 18) and grand composite curve (Fig. 19) demonstrate significant improvements in energy efficiency.

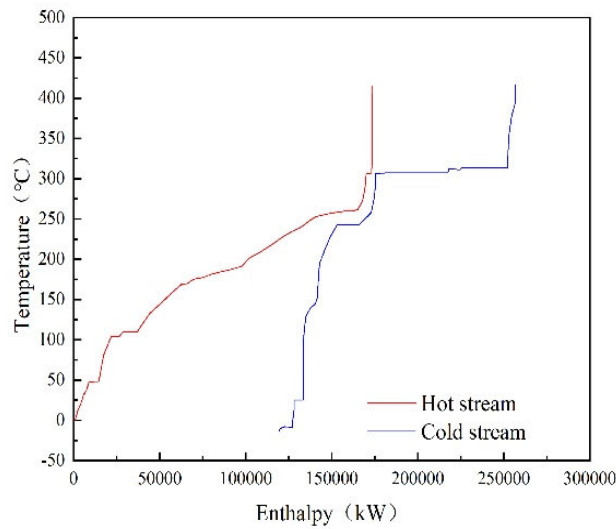


Figure 18. Process Composite Curve

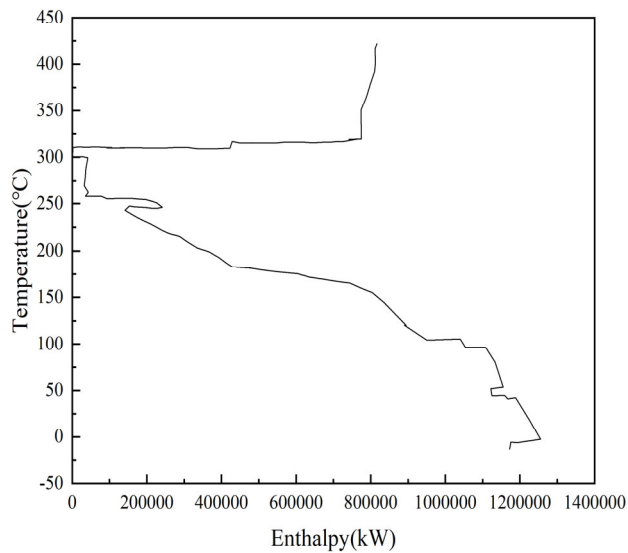


Figure 19. Overall combination curve diagram

The HEN design prioritized economic feasibility and operational simplicity. Among the Aspen-generated schemes

(Table 7), A_Design2 was selected for its low total cost (0.0114) and compact heat transfer area (403.1 m²).

Table 7. Recommended Heat Exchanger Network Scheme by the System

No.	Scheme	Total Cost (Cost/s)	Total Area (m ²)	Number of Units	Heating (kW)	Cooling (kW)	Selected
1	A_Design1	0.01458	1021	34	2362	3583	
2	A_Design2	0.0114	403.1	34	2362	3583	✓
3	A_Design3	0.0114	413.7	34	2362	3583	
4	A_Design4	0.01275	651.6	38	2362	3583	
5	A_Design5	0.01203	459.6	39	2362	3583	
6	Initial scheme	0.03077	3217	25	7261	8483	

The heat exchange network before optimization is shown in Fig. 20. As can be seen from Fig. 20, there are a large number of loop loops in this heat exchange network. Due to

the complexity of the heat exchange network, there are many loop loops, so the selected part is displayed, as shown in Fig. 21 and 22.

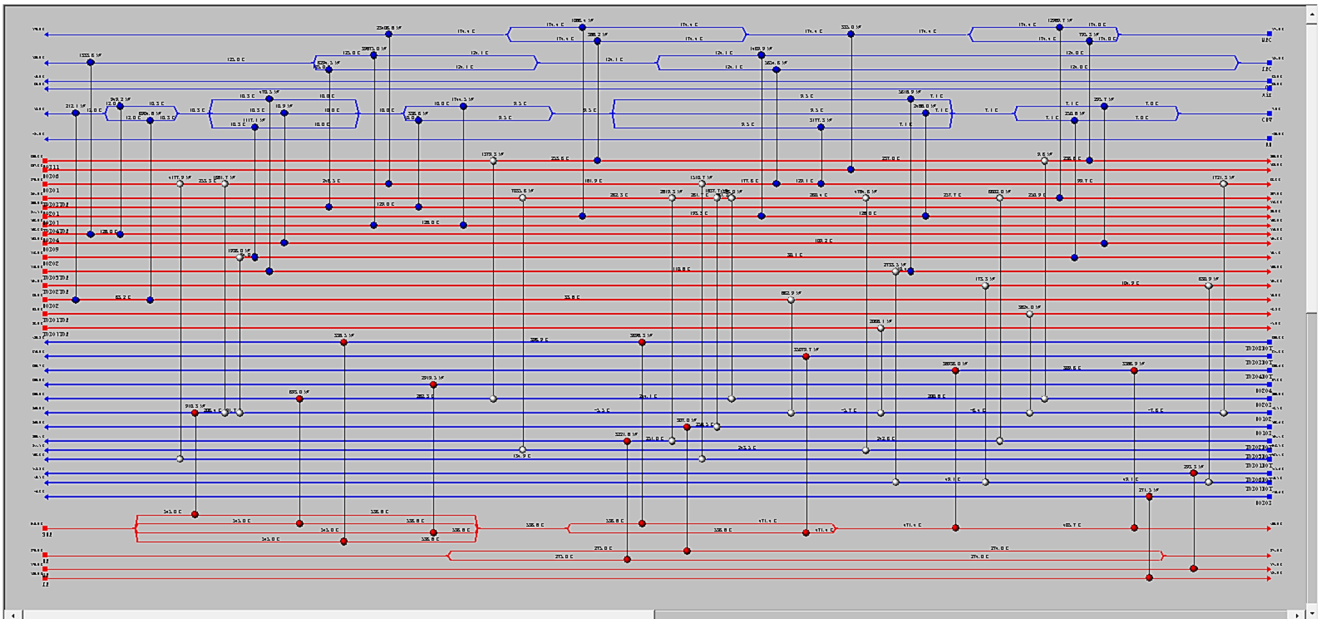


Figure 20. Heat exchanger network before optimization

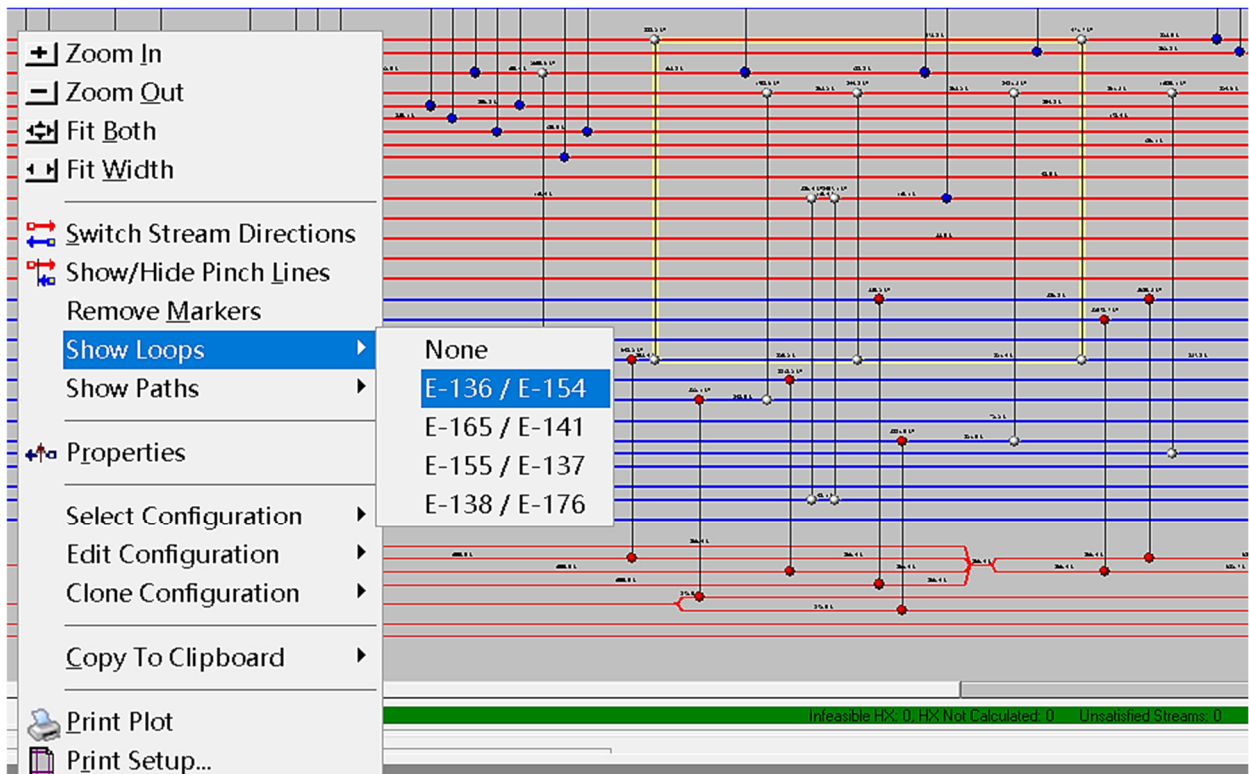


Figure 21. Loop Circuit

In actual operation, there is generally no loop, so the heat exchanger with small load or heat exchange area should be deleted, and it should be combined with other heat exchangers to break the loop and reduce the number of heat exchangers.

The optimized heat exchanger network (HEN) eliminated small-area and low-duty exchangers to enhance economic efficiency. Exchangers interfacing with multiple utilities or distant streams were removed to reduce piping complexity

and operational instability. The final design (Fig. 23) comprises 28 exchangers (including 3 internal units), achieving 5.91×10^5 kW of heat recovery while significantly lowering capital costs.

Before and after the process optimization and heat exchange network design of the original process flow, and before and after the use of the heat pump energy-saving technology, the use of public works is shown in Table 9.

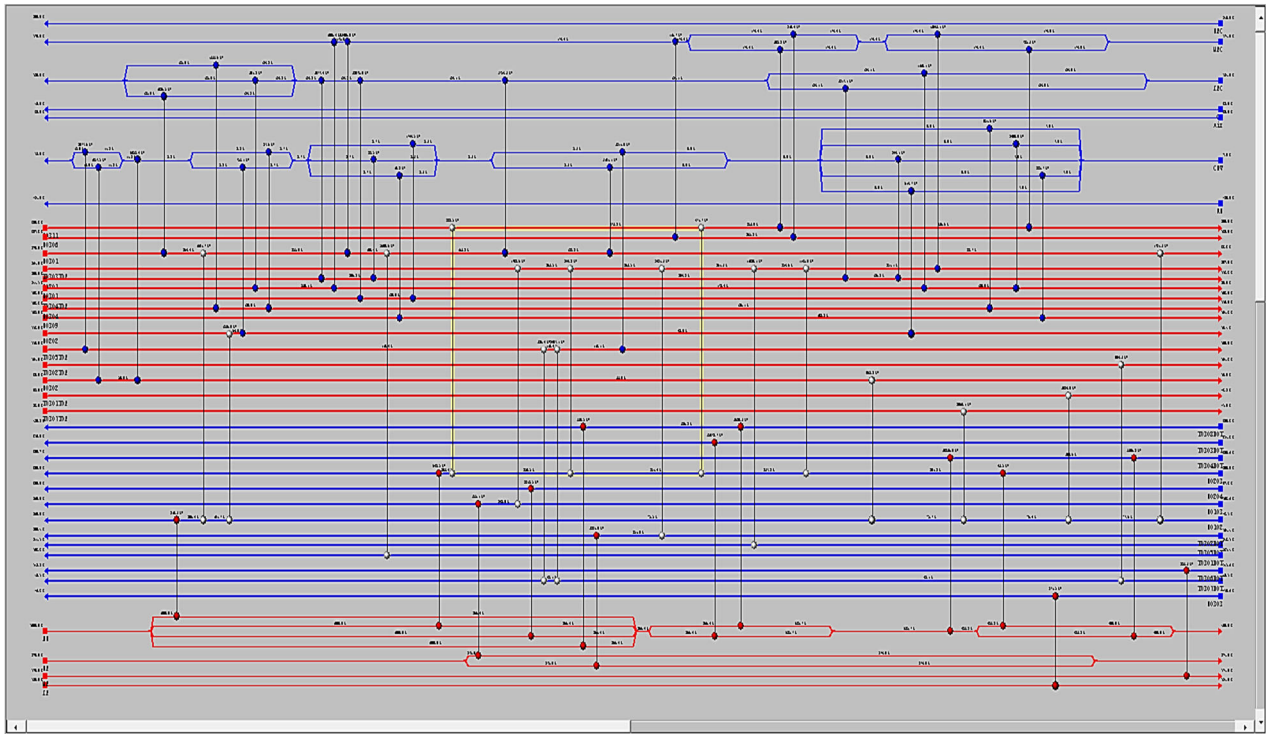


Figure 22. Loop Circuit

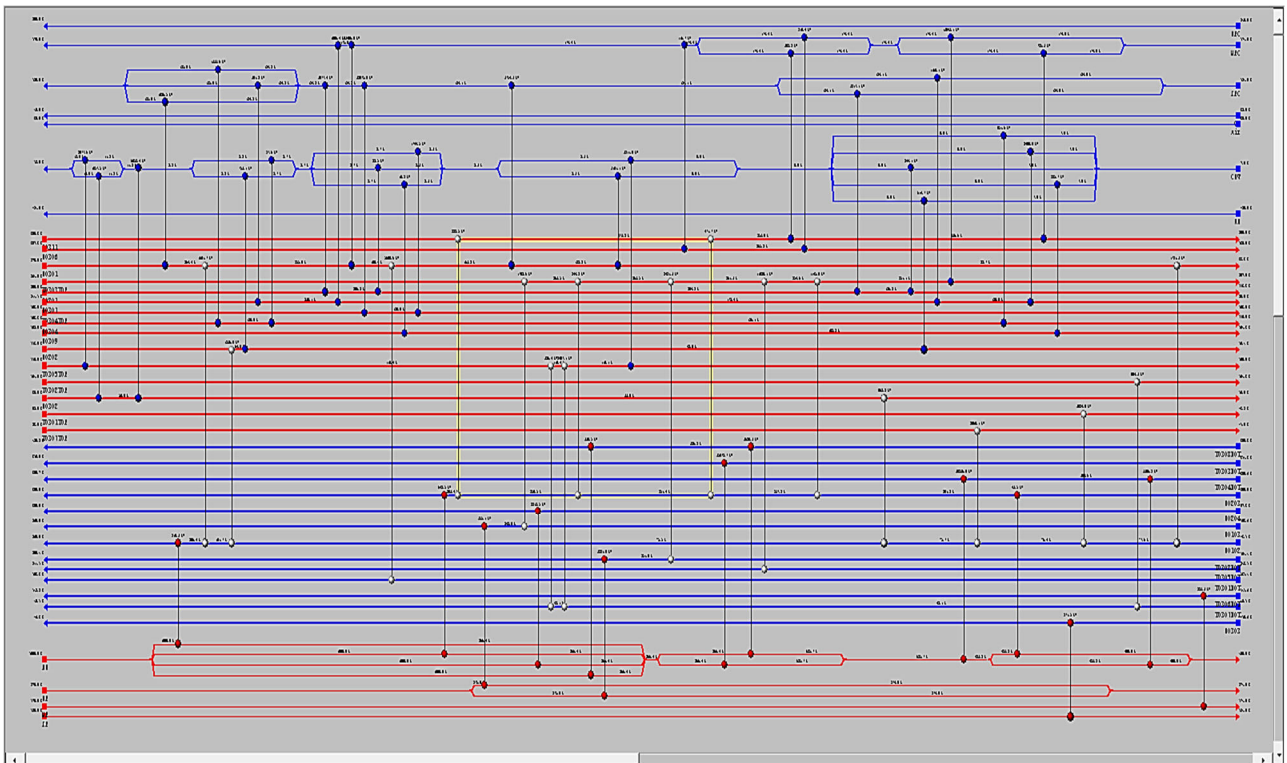


Figure 23. Optimized Heat Exchange Network

After optimization, 7.68×10^4 kW of cold and hot utilities can be saved. After optimization, the required hot utilities are 8.15×10^4 kW and the required cold utilities are 1.1817×10^5 kW. The cold public works used are circulating cooling water

and frozen water; The thermal utilities used are 124°C low pressure steam, 175°C medium pressure steam and 275°C high pressure steam.

Table 8. Heat exchanger utilities & inter-strand heat transfer distribution table

Exchanger	Type	Inlet/°C	Outlet/°C	Duty	Utility/Stream	
E0204	Cold	97.76	300	2919.49	SHP	/
E0103	Cold	193.56	260	2144.66	HP	/
E0203	Cold	200.54	300	3477.92	SHP	/
E0303	Cold	-15.56	-6.81	271.51	LP	/
E0102	Cold	-8.09	260	13004.38	HP	/
T0308BOT	Cold	350.28	420.19	4036.73	SHP	/
T0304BOT	Cold	309.55	309.65	42322.91	SHP	/
T0307BOT	Cold	49.06	49.11	3537.81	E0302	/
T0303BOT	Cold	314.27	315.46	35079.65	SHP	/
T0302BOT	Cold	194.40	259.43	12643.06	E0301	/
T0306BOT	Cold	141.62	142.24	293.30	MP	/
T0301BOT	Cold	131.36	153.25	5688.63	MP	/
T0305BOT	Cold	243.10	244.14	11820.15	T0303TOP	
E0306	Hot	307.77	180	335.04	LPC	
E0201	Hot	250	118.8	6631.100783	CW	
E0301	Hot	275	83.7954536	41330.41932	T0305BOT	CW
E0309	Hot	152.911517	104.831701	306.5693838	CE	
E0311	Hot	309.803606	200	2572.41187	MPC	
E0202	Hot	118.478862	19.416542	3303.841773	CHW	
E0307	Hot	244.140351	25	5044.310815	CHW	
E0302	Hot	80	10	7979.792653	T0307BOT	CHW
E0304	Hot	153.28	110	2282.823038	AIR	
T0304TOP	Hot	193.46	108.509236	41619.4716	CW	
T0303TOP	Hot	263.96	207.04263	37464.79089	T0305BOT	MPC
T0307TOP	Hot	27.98	-1.015085	2068.119683	RE	
T0302TOP	Hot	104.91	104.831275	5246.873857	CW	
T0305TOP	Hot	110.92	109.943756	8822.916312	CW	
T0301TOP	Hot	52.51	-3.2300731	3823.968231	RE	

Table 9. Utility information before and after optimization (including heat pump)

Parameter	Original Process	HEN Optimized	Without HPD	With HPD
Heating Utility/kW	143500	81500	2040.63	287.5
Cooling Utility/kW	188800	181700	2040.09	275.5
Total/kW	322300	263200	4080.7	576.1
Reduction/%	Heating Utility	43.21		85.9
	Cooling Utility	5.76		86.5
	Total	18.84		85.9

5. Conclusions

This study focuses on the preparation of adiponitrile (ADN) through adipic acid (AA) ammoniation and esterification-ammoniation methods. By employing full-process modeling, parameter optimization, and heat integration design, key bottlenecks in traditional processes—such as high energy consumption, excessive byproduct formation, and severe equipment corrosion—were systematically addressed. The main conclusions are as follows.

(1) Process route comparison and optimization potential

It has significant advantages in raw material availability (AA overcapacity in China) and safety (avoiding HCN highly toxic raw materials), but industrialization is limited by high temperature corrosion (>300°C), loss of phosphoric acid catalyst and high energy consumption. Through Aspen Plus process simulation and sensitivity analysis, the reactor residence time (541 seconds), temperature (250-260°C) and pressure (3.3bar) were optimized, the ADN yield was increased to 99.5%, and the by-product cyclopentanone production was reduced by 62%.

(2) Process energy-saving technology innovation and energy consumption optimization

AA catalytic ammonification method: The heat pump distillation technology is applied in the cyclopentanone refining tower (T0306), and the steam on the top of the tower is compressed and heated to drive the tower kettle reboiler. The energy consumption of cold/hot utilities is reduced by 86.5% and 85.9% respectively, and the total energy consumption of a single tower is reduced from 4080.7kW to 576.1kW.

(3) Global optimization of heat exchange network

AA catalytic ammonification method: First, Aspen Plus V11 and Aspen Energy Analyzer V11 were used to extract the original process flow data. After energy saving technology optimization and energy saving, the improved process flow was imported and the optimal scheme was selected for heat exchange network optimization design. After optimization, 7.68×104kW of cold and hot utilities can be saved. After optimization, the required hot utilities are 8.15×104kW and the required cold utilities are 1.1817×105kW. The number of heat exchangers was reduced from 34 to 28, including three internal heat exchangers.

Acknowledgements

This work was supported by the 2024 Liaoning Provincial Department of Education Basic Research Projects for Colleges and Universities [grant number LJ212410142155].

References

- [1] GUO X, LIU L, FENG H, et al. Flame retardancy of nylon 6 fibers: a review. *Polymers*, 2023, 15(9): 2161.
- [2] LIU Y, LI H J, YAO L F, et al. Synthesis process and properties of high-viscosity nylon 66. *New Chemical Materials*, 2024, 52(05): 125-132.
- [3] TOLMAN C A, MCKINNEY R J, SEIDEL W C, et al. ChemInform Abstract: Homogeneous Nickel-Catalyzed Olefin Hydrocyanation. *Cheminform*, 1986, 17(20).
- [4] BINI L, MUELLER C, VOGT D. Mechanistic studies on hydrocyanation reactions. *ChemCatChem*, 2010, 2(6): 590-608.
- [5] BINI L, MUELLER C, WILTING J, et al. Highly selective hydrocyanation of butadiene toward 3-pentenitrile. *Journal of the American Chemical Society*, 2007, 129(42): 12622-12623.
- [6] QI H L. Review on electrochemical synthesis of adiponitrile. *Chemical Industry Management*, 2016, (19): 116-117.
- [7] YUAN C, CHEN Y K, XU H C, et al. Aspen Plus simulation of the distillation unit for adiponitrile production via ammoniation of adipic acid. *Modern Chemical Research*, 2023, (21): 174-176.
- [8] PLASTICS INFORMATION EUROPE GROUP. China to lead world's capacity additions / India key contributor / Price pressure in Europe continues. *Plastics Information Europe*, 2024(TN.1151): 48.
- [9] CHEMICAL WEEKLY GROUP. BASF to stop adipic acid production at Ludwigshafen site in 2025. *Chemical Weekly*, 2024(7): 70.
- [10] CHEN Y, ZHOU H W, YU L, et al. Advances in non-petrochemical routes for adiponitrile synthesis. *Chinese Science Bulletin*, 2024, 69(03): 370-380.
- [11] ZHANG C C. Future development trends of China's nylon industry. *Tianjin Chemical Industry*, 2024, 38(1): 7-9.
- [12] OPPENHEIM J P, DICKERSON G L. Adipic acid. Hoboken: Kirk-Othmer Encyclopedia of Chemical Technology, 2000.
- [13] IWATA T. Biodegradable and bio-based polymers: Future prospects of eco-friendly plastics. *Angewandte Chemie*, 2015, 46(18): 3210-3215.
- [14] SLOBODINYUK A, SENICHEV V Y, PEREPADA M, et al. Structure and properties of urethane-containing elastomers based on adipic acid polyester and ethylene glycol, isophorone diisocyanate, and aromatic diamine. *Polymer Science, Series D*, 2023, 16(3): 576-581.
- [15] FENG C J. Preparation of high-efficiency low-cost platinum-based hydrogen oxidation gas diffusion electrodes and their application in adiponitrile electrosynthesis. Yancheng: Yancheng Institute of Technology, 2024.
- [16] PETROCHEMICAL NEWS GROUP. Invista concludes technology upgrade at its adiponitrile plant in Victoria. *PetroChemical News*, 2021, 59(13).
- [17] JAGADEESH R V, JUNGE H, BELLER M. Green synthesis of nitriles using non-noble metal oxides-based nanocatalysts. *Nature Communications*, 2014, 5(1): 4123.
- [18] BOLDYRYEV S, ILCHENKO M, KRAJAČIĆ G. Improving the economic efficiency of heat pump integration into distillation columns of process plants applying different pressures of evaporators and condensers. *Energies*, 2024, 17(4): 951.
- [19] RAMLI A L B. Modelling and optimizing single and multiple effect evaporators using Aspen Custom Modeler (ACM). Perth: Murdoch University, 2016.
- [20] HALL S G, LINNHOFF B. Targeting for furnace systems using pinch analysis. *Industrial & Engineering Chemistry Research*, 1994, 33(12): 3187-3195.
- [21] CHO J-H, WANG Y, CHEN R, et al. A survey on modeling and optimizing multi-objective systems. *IEEE Communications Surveys & Tutorials*, 2017, 19(3): 1867-1901.
- [22] QIAN B Z. China's first butadiene-based adiponitrile project put into operation. *Synthetic Materials Aging and Application*, 2022, 51(06): 162.
- [23] GAI X D, WANG Z W. Synthesis of reactive distillation process flowsheets. *Chemical Metallurgy*, 1998, (4): 332-338.
- [24] XU Z G, NI F C, NIU J S, et al. Method for synthesizing adiponitrile via high-temperature dehydration of liquid-phase ammoniated adipic acid: CN201911082334.7. 2023-02-03.
- [25] LI M Y. Response surface methodology for optimizing catalytic distillation parameters of ethyl acetate synthesis. Dalian: Dalian University of Technology, 2025.
- [26] CHEN C H. Energy-saving and emission-reduction transformation of coal chemical enterprises based on circular economy. Shanghai: East China University of Science and Technology, 2013.
- [27] WANG Y J, ZHU T, MA Z X, et al. Method for preparing adiponitrile by catalytic dehydration of adipamide: 202311348948. 2025-03-22.
- [28] FENG S P, CHENG D G, CHEN F Q, et al. Macrokinetics of adiponitrile synthesis via ammoniation of adipic acid. *CIESC Journal*, 2015, 66(8): 2890-2896.
- [29] BINI L, MUELLER C, WILTING J, et al. Highly selective hydrocyanation of butadiene toward 3-pentenitrile. *Journal of the American Chemical Society*, 2007, 129(42): 12622-12623.
- [30] DU L, CAO Z T, XU L, et al. Research progress in adiponitrile preparation methods. *Chemical Industry and Engineering Progress*, 2024, 1-20.
- [31] GAO F, ZHANG N Y, NAN L, et al. Reaction technology for adiponitrile synthesis (II): Study on side reactions. *Chemical Reaction Engineering and Technology*, 1991, (02): 128-135.
- [32] ZHANG N Y, GAO F, LU B, et al. Study on macrokinetics of adiponitrile synthesis. *Chemical Reaction Engineering and Technology*, 1989, (03): 1-9.
- [33] ROOSEN D I P, GRO D I B. Optimization strategies and their application to heat exchanger network synthesis. *Chemical Engineering & Technology*, 1996, 19(2): 185-191.
- [34] WANG Z B. Aspen Plus-based process simulation and heat exchanger network optimization of atmospheric and vacuum distillation units. Harbin: Harbin Institute of Technology, 2020.
- [35] LENG J, FAN S, DONG F L. Sustainable design and multi-objective optimization of heat pump assisted extractive distillation process for separating a ternary mixture of methyl acetate, tetrahydrofuran and methanol. *Journal of Cleaner Production*, 2023, 419: 138186.